Atomistic Design of Thermoelectric Properties of Silicon Nanowires

Trinh T.M. Vo, **Andrew J. Williamson**, and **Vincenzo Lordi**

Lawrence Livermore National Laboratory, Livermore, California 94550

Giulia Galli*

Department of Chemistry, University of California, Davis, California 95616

ABSTRACT

We present predictions of the thermoelectric figure of merit (*ZT*) of Si nanowires with diameter up to 3 nm, based upon the Boltzman transport equation and ab initio electronic structure calculations. We find that *ZT* depends significantly on the wire growth direction and surface reconstruction, and we discuss how these properties can be tuned to select silicon based nanostructures with combined n-type and p-type optimal *ZT*. Our calculations show that only by reducing the ionic thermal conductivity by about 2 or 3 orders of magnitudes with respect to bulk values, one may attain *ZT* larger than 1, for 1 or 3 nm wires, respectively. We also find that *ZT* of p-doped wires is considerably smaller than that of their n-doped counterparts with the same size and geometry.

Recent progress in nanomaterials synthesis has enabled the growth of semiconducting nanowires (NWs) with a range of sizes, growth directions, and surface structures.[1–5] These wires exhibit a significant size dependence of their electronic and optical properties,[6–9] and are attractive candidates for photovoltaic devices, photodetectors, field-effect transistors,[10,11] inverters,[12] light-emitting diodes, and nanoscale sensors.[13,14]

Among the numerous potential applications of silicon NW, recent studies have focused on their promise as thermoelectric (TE) materials with a so-called improved figure of merit (*ZT*).[15–17] The suitability of a system to convert heat into electricity and vice-versa is usually quantified in terms of *ZT*, which is defined as:

$$ZT = \sigma \frac{TS^2}{k_e + k_l} \qquad (1)$$

Here *S* is the Seebeck coefficient, σ is the electronic conductivity, and k_e, k_l are the electronic and lattice contributions to the thermal conductivity, respectively.

In the past decade, the search for materials with high *ZT* has been extremely challenging.[18] Recent experimental studies have suggested that the value of *ZT* may be significantly increased by incorporating nanostructures into bulk materials.[19] In particular, it has been proposed that at the nanoscale, quantum confinement may provide a mechanism for engineering systems with reduced electron and hole masses, and hence increased mobilities, which could lead to increased values of the electrical conductivity. Additionally, at the nanoscale, the large surface to volume ratio may increase the scattering of phonons by the surface and hence decrease the thermal conductivity (k_l) compared to bulk values, thus increasing *ZT*.[17,20–26] However, a mere size reduction and possible decrease in effective masses do not necessarily lead to an improved figure of merit; indeed, quantum confinement is expected to increase surface scattering of electrons, which may lead to a reduction of σ. Therefore, predicting nanoscale effects on thermoelectric properties requires quantitative calculations of σ, k_e, k_l, and *S* for specific systems and a thorough understanding of the interplay between electronic and ionic transport properties.

In this Letter, we report on a combination of density functional theory (DFT) and Boltzmann transport equation (BTE) calculations aimed at providing a microscopic description of the thermoelectric properties of silicon nanowires and to give insight into the key factors affecting the design of silicon based materials with *ZT* larger than 1.

We studied hydrogen terminated Si NWs grown along the [001], [011], and [111] directions with diameters up to 3 nm and surfaces with canted SiH_2 dihydrides and (2×1) reconstructions.[27] The relaxed atomic and band structures for each Si NW were calculated using DFT.[28] The electronic energies and velocities, the electrical conductivity σ, the electronic contribution to the thermal conductivity, k_e, and the Seebeck coefficient, *S*, were then obtained from the solution of the one-dimensional Boltzman transport equation (BTE) in the constant-relaxation-time approximation (RTA):

* Corresponding author. E-mail: gagalli@ucdavis.edu.

$$\sigma = \Lambda^{(0)}$$
$$k_e = \frac{1}{e^2 T}[\Lambda^{(2)} - \Lambda^{(1)}(\Lambda^{(0)})^{-1}\Lambda^{(1)}],$$
$$S = \frac{1}{e^2 T}(\Lambda^{(0)})^{-1}\Lambda^{(1)}, \text{ where} \qquad (2)$$
$$\Lambda^{(\alpha)} = e^2 \tau \int \frac{d\mathbf{k}}{\pi}(-\frac{\partial f}{\partial \epsilon})\upsilon(\mathbf{k})\upsilon(\mathbf{k})(\epsilon(\mathbf{k}) - \mu)^{\alpha}$$

Here e is the charge of carriers, T is the temperature, $f(\epsilon)$ is the Fermi distribution function, $\epsilon(\mathbf{k})$ is the energy associated with a given wave vector $\mathbf{k}$, τ is the relaxation time, $\upsilon(\mathrm{k})$ is the group velocity, and μ is the electron chemical potential. The velocity $\upsilon(\mathbf{k})$ is calculated from the band structure: $\upsilon = (1/h)(\partial\epsilon(\mathbf{k})/\partial\mathbf{k})$. We assumed that transport in Si NWs occurs in a diffusive regime, and σ, S, and k_e were evaluated by considering only elastic scattering processes. Inclusion of nonelastic scattering would require the use of approaches beyond the RTA. We note that Gilbert et al.,[29] have recently suggested that transport is expected to switch from ballistic to diffusive in Si NWs longer than 1.4 nm. The systems considered here represent macroscopically long wires, as periodic boundary conditions in the growth direction were used in our calculations.

The relaxation time, τ, is a complex function of the atomic structure, electron energy, temperature, and carrier concentrations. In systems with low doping and low carrier concentrations, τ is mostly limited by phonon scattering. For high doping and carrier concentrations, τ is mainly limited by impurity scattering. The goal of our work is to determine the qualitative effect of a Si NW's growth direction and surface structure on its TE figure of merit. Therefore, the values of τ were obtained by fitting the mobility, calculated using eq 2, to measured carrier concentration dependent mobility data of bulk Si.[30] To test the validity of this approximation, we estimated the difference in mobilities between NWs and bulk Si by performing ab initio, DFT calculations of scattering rates for representative samples of boron doped bulk Si, and of a 1.1 nm NW, with a carrier concentration of $\sim 8 \times 10^{20}$ cm^{-3} and B in the interior of the NW. We followed the procedure outlined in ref 31. For constant τ, one has: $\tau^{-1} \propto |T_m|^2$, where $|T_m|$ is a scattering matrix element and E_{DOS} is the joint density of states for the transition contributing to $|T_m|$. We found that intravalley scattering at the band extrema is dominant for both the NW and the bulk, and we therefore approximated $|T_m|$ with its value at the band extremum, using the Born approximation, and we calculated the average E_{DOS} over 5 $k_B T$ (here T is the temperature and k_B the Boltzmann constant). We obtain $\tau_{\mathrm{wire}}/\tau_{\mathrm{bulk}} \approx 1$–4, thus confirming the intuitive expectation of larger relaxation times in a small nanowire with respect to bulk values. These results show that using values of the relaxation time extrapolated from those of the bulk is a reasonable approximation to obtain trends and qualitative estimates; the use of bulk values possibly underestimates the calculated values of ZT that depends linearly on τ in the constant relaxation time approximation.

Figure 1 shows σ, S and k_e for a 1 nm wire as a function of electron and hole concentration; the carrier concentration n, is defined as $n = \int d\epsilon N(\epsilon)f(\epsilon)$, where $N(\epsilon)$ is the electronic density of states. In this model, n represents the concentration
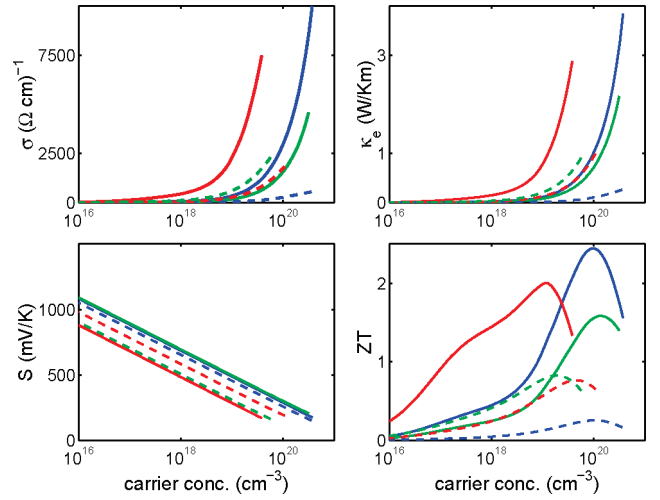
Figure 1. Calculated electronic conductivity (σ), electronic part of the thermal conductivity (k_e), Seebeck coefficient (S), and figure of merit (ZT) of p-type (dashed lines) and n-type (solid lines) doped 1.1 nm Si NWs grown along the [001] (blue), [011] (red), and [111] (green) directions.

of charge carriers in a system that is artificially doped by varying the chemical potential while assuming a fixed band structure. Both σ and k_e increase as more carriers are available to transport charge and heat, while the Seebeck coefficient decreases with increasing carrier concentration, in the absence of electron–phonon interaction. In addition to an expected dependence on carrier concentration, σ, k_e, and S show a strong dependence on growth direction arising from differences in the band structure. For example, for 1 nm Si NWs grown in the [011] direction, the conduction band minimum (CBM) is highly dispersive and the electronic states are delocalized in the direction parallel to the wire axis. In contrast, the CBMs in the [001] and [111] Si NWs are oriented in the direction diagonal and perpendicular to the NW axis, respectively, and the band structures are much flatter (see ref 28). Consequently, the 1 nm [011] Si NWs have the lowest effective mass and highest values of σ and k_e for a given carrier concentration. Therefore if one is only interested in selecting wires of about 1 nm diameter with the highest electrical conductivity, our simulations predict that the [011] growth direction is the most promising. On the other hand, for 3 nm wires, it is the [001] growth direction that exhibits the highest σ (not shown). In 3 nm NWs, even though the CB of the [011] direction is more dispersive than that of the [001] (resulting in a smaller effective mass), a higher degree of degeneracy is observed for [001] and therefore more bands contribute to determining the value of the conductivity.

Having calculated σ, S and k_e, we can now establish how much the thermal conductivity needs to be lowered, with respect to that of bulk Si, in order to obtain ZT larger than 1. At present, there is no consensus in the literature about computed values of ionic thermal conductivity for Si NWs; however, it appears that shape and surface structure, in addition to and possibly more importantly than size, may lead to a decrease of thermal conductivity with respect to bulk values.[32] Furthermore, it is possible that other effects
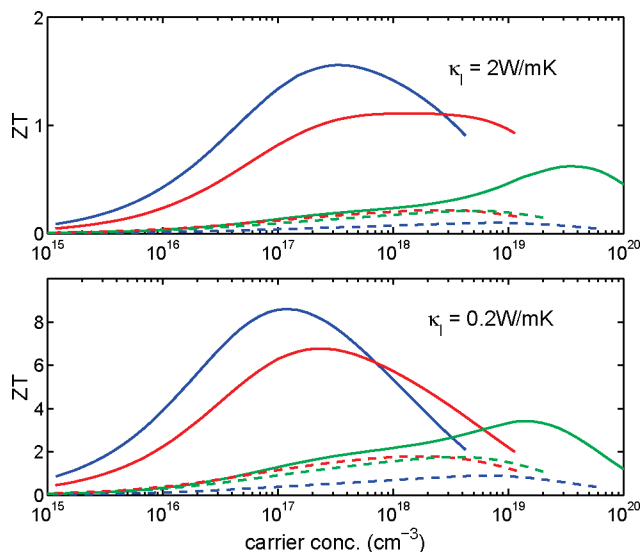
Figure 2. Values of the figure of merit (*ZT*) of 3.0 nm Si NWs computed assuming $k_l = 2$ W/mK (upper panel) and $k_l = 0.2$ W/mK (lower panel); we show three growth directions [001] (blue), [011] (red), and [111] (green) with canted surface structures (see text). The solid and dash lines denote n-type and p-type systems, respectively.

such as wire−wire interaction[33] and electron–phonon interaction[34] might be responsible for a decrease of thermal conductivity at the nanoscale. Figure 2 shows *ZT* for 3 nm wires computed assuming $k_l = 2$ W/mK and $k_l = 0.2$ W/mK, respectively. Preliminary results[32,36] obtained using molecular dynamics simulations indicate a weak dependence of the ionic thermal conductivity on growth direction, much weaker, e.g., than on surface structure and morphology; therefore, here the values of k_l have been taken as constant, as a function of the growth direction. The *ZT* for 1 nm wires assuming $k_l = 2$ W/mK is shown in Figure 1. This value of k_l[35,37] corresponds to some of the values proposed in the literature for small wires and is indicative of the order of magnitude required to have both n-doped and p-doped wires with *ZT* larger than 1 for sizes of about 1 nm. The value of 0.2 W/mK is instead representative of the value required at 3 nm in order to have *ZT* larger than 1, and it represents a dramatic reduction of 3 orders of magnitudes with respect to the bulk value.

Our results show that the strong dependence of electronic properties (σ, S, and k_e) on growth direction and surface reconstruction may be tuned to vary *ZT* by more than a factor of 2 for fixed values of the ionic thermal conductivity. However, the ultimate challenge, in order to reach *ZT* higher than 1, resides in lowering the thermal conductivity by 2–3 orders of magnitudes with respect to bulk values. Very recent experimental results indicate that such a decrease is possible,[34,35] and thus Si NWs may become very promising systems for use in thermoelectric applications.

In addition to a given growth direction, for each wire size, there is an optimal carrier concentration yielding the maximum attainable value of *ZT*. Figures 1 and 2 show that *ZT* initially increases with carrier concentration as σ increases. At higher carrier concentrations, the increase of k_e and decrease of S results in a net decrease of *ZT*. Therefore,

for example, for the 1.1 nm wires shown in Figure 1, these optimal carrier concentrations vary between 10^{18} and 10^{20} cm^{-3}, producing maximum *ZT* values ranging from 0.25 to 2.5. For 3 nm wires (Figure 2), the maximum *ZT* values vary from 0.16 to 1.55 for concentrations between 10^{17} and 10^{20} cm^{-3} and values of k_l of about 2 W/mK (see Figure 2). Our results show that when optimizing materials parameters for Si NWs with high *ZT*, in addition to selecting an optimal growth direction, one should also consider the level of doping required to achieve a given *ZT* value. For example, 1 nm [001] Si NWs have a higher n-type *ZT* value of 2.5 compared to 2.0, found for the [011] direction; however, a carrier concentration of 1×10^{20} cm^{-3} is required to achieve it, compared to only 1×10^{19} cm^{-3} for the [011] case. Given that the maximum doping concentration obtainable in bulk Si is of the order of 10^{21} cm^{-3}, reaching a doping level of 10^{20} cm^{-3} in a 1 nm Si NW may be very challenging. Therefore, from a practical point of view, for 1 nm NWs, the [011] growth direction appears to be the best candidate for TE materials. For 3 nm NWs, on the other hand, the [001] direction turns out to be the best candidate for n-doped systems because it has the highest *ZT*, which occurs at a much lower concentration than that of the 1 nm case (see Figure 2). For p-type wires, [011] is instead a better choice.

We note that, in order to build an efficient TE device, one needs to combine p- and n-type wires into a parallel structure such as that proposed by Mujamdar et al.[19] The maximum overall *ZT* for such a structure can be obtained by using NWs with appropriate doping types (n- or p-type), concentration, and growth direction. For instance, combining the n-type [011] with a doping concentration corresponding to the max *ZT* (1×10^{19}) and p-type [111] with a doping concentration of 2×10^{19} will yield a device *ZT* value of 1.16 (see Figure 1) for 1 nm wires. However, for 3 nm wires (see Figure 2), it is the combination of n-type [001] and p-type [011] that appears to yield the highest value of *ZT* (0.46) for $k_l = 2$ W/mK. We note that for the same values of the ionic thermal conductivity, an increase of diameter from 1 to 3 nm leads to a decrease of optimal *ZT* by about a factor of 2. It also leads to much more pronounced differences between *ZT* values of n-doped and p-doped systems.

Finally, we examined the dependence of *ZT* on the surface structure of the Si NWs. Figure 3 compares *ZT* for n-type Si NWs with canted dihydride and (2 × 1) reconstructed surface structures. The NW diameter of 1.2 nm is used for the case of [111] because NWs with smaller diameters do not exhibit surface reconstructions. For 1.1 and 1.2 nm [001] and [111] wires (see Figure 3), the surface reconstruction produces a small band splitting at the conduction band minimum.[28] This results in a partial occupation of the higher energy bands, leading to a larger value of k_e and hence a smaller maximum value of *ZT*. In the case of [011] wires, there is a large splitting between the first and second conduction bands, for both canted and reconstructed surfaces, so the maximum value of *ZT* is relatively unaffected by the surface reconstruction. For 3 nm NWs (see Figure 3), the concentrations at which the maximum *ZT* value occurs for the canted and reconstructed surfaces are markedly different.
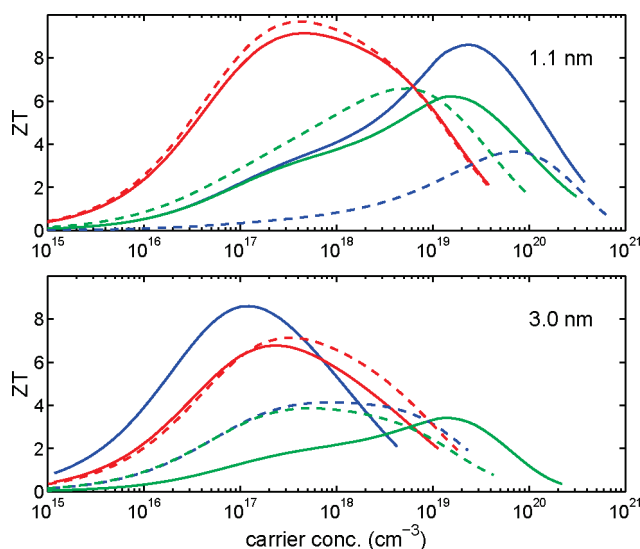
Figure 3. Figure of merit (*ZT*) as a function of carrier concentration for n-type Si NWs with two different surface structures (canted: solid lines; (2 × 1) reconstructed: dashed lines), and the three growth directions [001] (blue), [011] (red), and [111] (green). NW diameter is 1.2 nm for the [111] direction.

The difference is largest for the [001] direction. These results emphasize the need to optimize not only the band gap, but also band splittings and effective masses of a given material, in order to optimize its value of *ZT*.

In conclusion, we have employed a combination of first-principles electronic structure and Boltzmann transport calculations to predict the thermoelectric figure of merit of silicon nanowires up to 3 nm. Although most of Si NWs discussed in the experimental literature have diameter equal to or larger than 10 nm, very recent reports[5] have shown that the fabrication of wires with a diameter as small as 1.6 nm is possible. Our results show that Si NWs may become good candidates for fabricating thermoelectric materials, provided the ionic thermal conductivity can be decreased by several orders of magnitude with respect to the bulk (up to 3), and very recent experiments indicate this is now within reach.[34,35] We showed that by changing the growth direction and NW diameter, or by tuning the surface structure via chemical etching or heat treatment, it is possible to tune the Si NWs figure of merit. In principle, it should also be possible to further optimize NW thermoelectric properties by alloying silicon with other elements, such as germanium, and by functionalizing surfaces of NWs, and we are currently investigating these possibilities. The type of calculation reported in this work can be extended to a variety of nanoscale materials, including compound nanostructures, and represent a valuable investigation tool to study trends in thermoelectric properties at the nanoscale.

References

(1) Sharama, S.; Kamin, T.; Williams, R. *Appl. Phys. A* **2005**, *80*, 1225.
(2) Zhang, Y.; Tang, Y.; Wang, N.; Lee, C.; Bello, I.; Lee, S. *J. Cryst. Growth* **1999**, *197*, 136.
(3) Yan, X.; Liu, D.; Ci, L.; Wang, J.; Zhou, Z.; Yuan, H.; Song, L.; Gao, Y.; Liu, L.; Zhou, W.; Wang, G.; Xie, S. *J. Cryst. Growth* **2003**, *257*, 69.
(4) Hochbaum, A.; Fan, R.; He, R.; Yang, P. *Nano Lett.* **2005**, *5*, 457.
(5) Padova, P.; Quaresima, C.; Perfetti, P.; Olivieri, B.; Leandri, C; Aufray, B.; Vizzini, S.; Lay, G. *Nano Lett.* **2008**, *8*, 271.
(6) Canham, L. *Appl. Phys. Lett.* **1990**, *57*, 1046.
(7) Katz, D.; Wizansky, T.; Milo, O. *Phys. Rev. Lett.* **2002**, *89*, 86801.
(8) Duan, X.; Wand, J.; Lieber, C. *Appl. Phys. Lett.* **2000**, *76*, 1116.
(9) Ma, D.; Lee, C.; Au, C.; Tong, S.; Lee, S. *Science* **2003**, *299*, 1874.
(10) Duan, X.; Huang, Y.; Cui, Y.; Wang, J.; Lieber, C. *Nature* **2001**, *409*, 66.
(11) Cui, Y.; Zhong, Z.; Wang, D.; Wang, W.; Lieber, C. *Nano Lett.* **2003**, *3*, 149.
(12) Cui, Y.; Lieber, C. *Science* **2001**, *291*, 851.
(13) Hahm, J.; Lieber, C. *Nano Lett.* **2004**, *4*, 51.
(14) Cui, Y.; Wei, Q.; Park, H.; Lieber, C. *Science* **2001**, *293*, 1289.
(15) Abramson, A.; Kim, W.; Huxtable, S.; Yan, H.; Wu, Y.; Majumdar, A.; Tien, C.; Yang, P. *J. Microelectromech. Syst.* **2004**, *13*, 505.
(16) Dresselhaus, M.; Dresselhauss, G.; Sun, X.; Zhang, Z.; Cronin, S.; Koga, T. *Phys. Solid State* **1999**, *41*, 679.
(17) Kubakaddi, S.; Mulimani, B. *J. Appl. Phys.* **1985**, *58*, 3643.
(18) Majumdar, A. *Science* **2004**, *303*, 777.
(19) Majumdar, A. *J. Microelectromech. Syst.* **2004**, *13*, 505.
(20) Hicks, L. *Appl. Phys. lett.* **1993**, *63*, 3230.
(21) Hicks, L.; Dresselhaus, M. *Phys. Rev. B* **1993**, *47*, 16631.
(22) Sun, X.; Zhang, Z.; Dresselhaus, M. *Appl. Phys. Lett.* **1999**, *74*, 4005.
(23) Rabin, O.; Lin, Y.; Dresselhaus, M. *Appl. Phys. Lett.* **2001**, *79*, 81.
(24) Khitun, A.; Balandin, A.; Wang, K. *Superlattices Microstruct.* **1999**, *26*, 181.
(25) Hicks, L.; Dresselhaus, M. *Phys. Rev. B* **1993**, *47*, 12727.
(26) Hicks, L.; Harman, T.; Sun, X.; Dresselhaus, M. *Phys. Rev. B* **1996**, *53*, 10493.
(27) In a previous work,[28] we showed that Si NW with surfaces terminated by symmetric SiH$_2$ dihydrides are metastable, therefore we do not consider those geometries here.
(28) Vo, T.; Williamson, A.; Galli, G. *Phys Rev B* **2006**, *74*, 045116.
(29) Gilbert, M.; Akis, R.; Ferry, D. *J. Appl. Phys.* **2005**, *98*, 094303.
(30) Jacoboni, C.; Canali, C.; Ottaviant, G.; Quaranta, A. *Solid-State Electron.* **1977**, *20*, 77.
(31) Evans, M.-H.; Zhang, X.-G.; Joannopolos, J.; Pantelides, S. *Phys. Rev. Lett.* **2005**, *95*, 106802.
(32) Reed, J.; Williamson, A. J.; Schwegler, E.; Galli, G. manuscript in preparation.
(33) Donandio, D.; Galli, G. *Phys. Rev. Lett.* **2007**, *99*, 255502.
(34) Bukai, A.; Bunimovich, Y.; Kheli, J.; Yu, J.; Goddard, W.; Heath, J. *Nature* **2007**, *2007*, 168.
(35) Hochbaum, A.; Chen, R.; Delgado, R. D.; Garnett, E.; Majumdar, A.; Yang, P. *Nature* **2007**, *45*, 163.
(36) Donandio, D.; Galli, G. manuscript in preparation.
(37) Mingo, N.; Yang, L.; Li, D.; Majumdar, A. *Nano Lett.* **2003**, *3*, 1713.

NL073231D